J Neurosurg 115:624–632, 2011

Crescent sign on magnetic resonance angiography revealing incomplete stent apposition: correlation with diffusion-weighted changes in stent-mediated coil embolization of aneurysms

Clinical article

Robert S. Heller, B.S.,[1,3] William R. Miele, M.D.,[1,3] Daniel D. Do-Dai, M.D.,[2,3] and Adel M. Malek, M.D., Ph.D.[1–3]

[1]Cerebrovascular and Endovascular Division, Department of Neurosurgery, [2]Department of Radiology, Tufts Medical Center; and [3]Tufts University School of Medicine, Boston, Massachusetts

Object. Few data are available on how closely stents appose the luminal vessel wall in stent-mediated coil embolization of intracranial aneurysms and on the effect of incomplete stent apposition on procedural thromboembolic complications.

Methods. Postprocedural 3-T MR diffusion-weighted imaging and time-of-flight angiography were obtained in 58 patients undergoing stent-mediated coil embolization of aneurysms using the Enterprise closed-cell and Neuroform open-cell self-expanding intracranial microstents.

Results. A distinctive semilunar signal pattern, identified using 3-T MR angiography, represented flow outside the confines of the stent struts in patients in whom Enterprise but not Neuroform devices were used. This pattern, designated as the crescent sign, was confirmed to correspond to incomplete stent apposition by use of high-resolution angiographic flat-panel CT scanning revealing flow ingress into and egress out of the isolated luminal wedge. The presence of the crescent sign was seen in 18 of 33 Enterprise-treated but in 0 of 25 Neuroform-treated cases, and was more likely in stents delivered in the tortuous internal carotid artery ($p = 0.034$). The crescent sign was strongly predictive of ipsilateral postprocedural lesions seen on diffusion-weighted imaging in the entire population (OR 18, 95% CI 4.33–74.8; $p < 0.0001$). In the Enterprise stent subset, ipsilateral lesions were detected on diffusion-weighted imaging in 15 (45%) of 33 cases; the crescent sign was seen in 12 (80%) of 15 patients with ipsilateral lesions on diffusion-weighted imaging, but in only 6 of 18 patients without lesions (OR 8, 95% CI 1.61–39.6; $p = 0.006$).

Conclusions. Incomplete stent apposition is detectable on 3-T MR angiography as a crescent sign, and was found to be highly prevalent in Enterprise closed-cell design stents used to assist coil embolization of aneurysms. Incomplete stent apposition was also associated with periprocedural ipsilateral hyperintense lesions on diffusion-weighted imaging. These results identify an association between incomplete stent apposition and thromboembolic complications in stent-mediated coil embolization of intracranial aneurysms. *(DOI: 10.3171/2011.4.JNS102050)*

Key Words • **aneurysm** • **magnetic resonance imaging** • **intracranial stent** • **coil embolization** • **interventional neurosurgery** • **vascular disorders**

Stent-mediated coil embolization relies on placement of an intracranial stent across the neck of an aneurysm to serve as a supportive scaffold preventing coil herniation into the parent vessel (Fig. 1A). Relying on predominantly 2 types of self-expanding microstents—the open-cell design Neuroform, and the newer, more maneuverable closed-cell design Enterprise (Fig. 1B)—stent-mediated coil embolization is becoming increasingly prevalent in the endovascular treatment of wide-necked aneurysms.[7] Although in vitro evaluation performed using angiographic flat-panel CT scans has revealed crimping and ovalization on bending of these intracranial stents in elastic tube models[2,6] (Fig. 1C), there are few in vivo data on intracranial stent-strut to vessel wall apposition, even after 8 years of clinical use.[10,12,15,21]

Abbreviations used in this paper: ACT = activated clotting time; BMI = body mass index; ICA = internal carotid artery.

This article contains some figures that are displayed in color online but in black and white in the print edition.

Brought to you by Tufts University | Unauthenticated | Downloaded 11/15/26 12:59 PM UTC

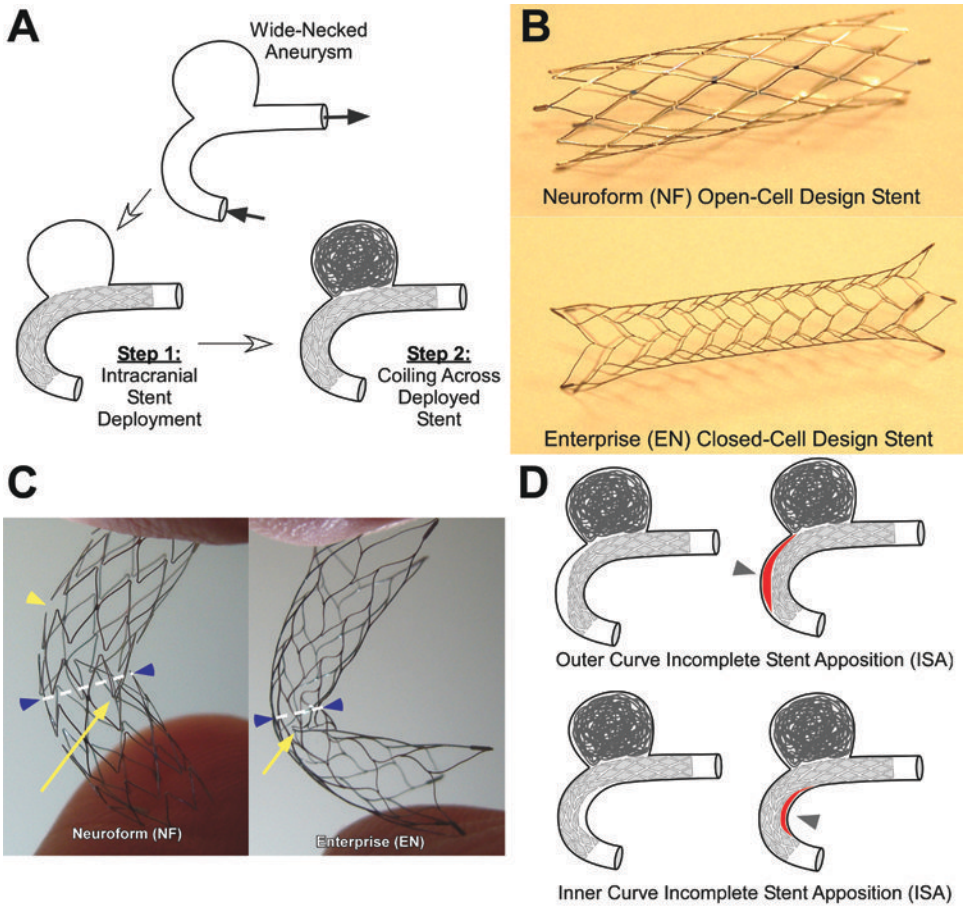


Fig. 1. **A:** Schematic illustration of steps involved in stent-assisted coil embolization of a wide-necked aneurysm with good vessel wall/stent apposition. **B:** Two types of intracranial stents for stent-assisted coil embolization of aneurysms: the open-cell design Neuroform and the lower-profile, closed-cell design Enterprise. **C:** Simple manual bending highlights the different behavior of closed- and open-cell design stents: inner curve fish-scaling *(arrow)* and outer flaring with increased gap in the Neuroform device *(yellow arrowhead)*; inner crimp *(arrow)* and ovalization with diameter loss in the Enterprise device *(dashed line)*. **D:** Incomplete stent apposition *(arrowheads)* can occur on either the inner or outer curve of a vessel where the stent struts fail to maintain contact with the vessel wall.

This is partly the result of the poor ability of conventional catheter-based or CT angiography to resolve < 65-μm-thick nitinol struts of intracranial stents from the vessel wall within the bony confines of the skull. In contrast, incomplete stent apposition has been widely studied in the treatment of coronary and carotid artery stenosis[4,17] (Fig. 1D).

With the increased use of stent assistance in the adjunctive embolization of wide-necked intracranial aneurysms,[7,20] evaluating the presence of incomplete stent apposition in the cerebral circulation and studying its link to thromboembolic events are important steps in elucidating possible sources of procedural complications. Prior work on stent-assisted coil embolization has focused on identification of adverse clinical events,[14,15] with less attention to acute ischemic lesions that can be detected by MR-based diffusion-weighted imaging.[3] Such use of diffusion-weighted imaging following aneurysm coil occlusion has previously been successful in confirming the protective effect of pretreatment with antiplatelet inhibitors and in modifying treatment protocols to decrease procedural thromboembolic complications.[5,8,18] Concomitantly, recent advances in higher field strength (3-T) MR and flat-panel CT imaging have led to increased spatial resolution and provided greater clarity of stent-related structures.[6,16]

In this study, we used multimodality imaging to identify and characterize the presence of an orphaned area of semilunar flow visible on 3-T MR angiography outside the confines of the stent strut susceptibility signal drop. This MR imaging–based crescent sign was confirmed to be the result of a lack of apposition between stent struts and the vessel wall through the use of flat-panel CT imaging. The clinical value of this incomplete stent apposition indicator as a predictor of procedure-related thromboembolic complications was evaluated using simultaneous postprocedural diffusion-weighted imaging in a prospectively collected patient cohort undergoing stent-assisted coil embolization of intracranial aneurysms.

Methods

Patient Selection

All patients undergoing stent-mediated coil emboli-

Brought to you by Tufts University | Unauthenticated | Downloaded 11/15/26 12:59 PM UTC

zation of ruptured and unruptured intracranial aneurysms between January 2009 and July 2010 underwent prospective postprocedural 3-T diffusion-weighted imaging and MR angiography. Patient age, sex, BMI, aneurysm location, rupture status, and aneurysm size were analyzed in addition to comorbid conditions including the following: hypertension, diabetes mellitus, hyperlipidemia, coronary artery disease, peripheral vascular disease, prior myocardial infarction, and a history of or current tobacco and alcohol use. Patients' use of medications was also analyzed, including preprocedural dual antiplatelet inhibition with aspirin and clopidogrel, proton pump inhibitor use, and intraprocedural intravenous heparin and clotting function via ACT measurement. The use of the Neuroform and Enterprise stents and the procedures in the current study were approved by the institutional review board.

Procedure in Detail

Patients were pretreated with clopidogrel (75 mg by mouth daily) and aspirin (325 mg by mouth daily) for at least 3 days prior to the procedure. Femoral access was either unilateral or bilateral, depending on the method and type of stent used. The same calibrated flat-panel biplanar Siemens Artis digital subtraction angiography system was used for all procedures. The 3D rotational angiography and angiographic flat-panel CT (DynaCT) acquisitions were reconstructed and analyzed according to the manufacturer's directions by use of the Leonardo software package (Siemens).

Two endovascular techniques were used: in the sequential technique, the stent is first delivered via its own microcatheter delivery system, then a separate microcatheter is used to catheterize the aneurysm dome through the stent interstices, and coil insertion is then performed. In the jailing technique, the aneurysm is first selected by the microcatheter intended for coil placement, followed by stent delivery, jailing the first microcatheter in the dome, through which coil insertion then proceeds. In the sequential technique, a 5 Fr guide catheter was used in most cases; in the jailing technique, a similar 6 Fr guider was used in most cases treated with Enterprise devices and 2 (bifemoral access) 5 Fr guiders (Envoy guide catheters, Cordis) were used for Neuroform-treated cases.

Patients received anticoagulation therapy with intravenous heparin to a target ACT of > 230 seconds prior to cervical advancement of the guider into the target vessel. All guiders and microcatheters were continuously irrigated with heparinized saline solution (1 USP unit heparin/ml). A Prowler Plus Select microcatheter (Codman) was navigated into position with the aid of a Synchro-2 0.014-in microwire (Boston Scientific) and was used to deliver the Enterprise stent in standard fashion per the manufacturer's instructions for use; although the Enterprise can be retrieved and repositioned by design, there were no instances of stent resheathing or repositioning in this series. A Neuro Renegade microcatheter (Boston Scientific) was used to deposit the Neuroform stent by using the stent transfer technique according to manufacturer's instructions for use. All patients remained on intravenous anticoagulation therapy for a target partial thromboplastin time of 55–70 seconds for 24 hours following the procedure, and were maintained on daily aspirin (325 mg) and clopidogrel (75 mg) by mouth for the first 3 months following the procedure.

Stent selection prior to delivery was based on preoperative analysis of target vessel anatomy and consideration of the advantages of a stent type in certain circumstances, such as the ability of dual Neuroform stents to be delivered in a Y construct in the posterior circulation, or the greater flexibility of the Enterprise stent when navigating tortuous vasculature. The 2 stents were otherwise considered to be equivalent in their ability to buttress the coil mass and prevent herniation into the parent vessel. These preferences are evidenced by the high proportion of Enterprise stents used in the anterior circulation and intracranial ICA.

Angiographic Analysis and MR Imaging Methods

Angiographic studies were analyzed for aneurysm location and size, size and number of guide catheters used, and endovascular technique. During the study period, all patients underwent 3-T MR diffusion-weighted imaging and MR angiography of the brain within 3 days of the initial procedure; a 3-T Achieva unit (Philips Medical Systems) was used. The MR angiography study was obtained using a 3D time-of-flight technique, with TR 25 msec, TE 3.45 msec, flip angle 20°, 20-cm field of view, with 1-mm phase encoding, reconstructed to 512 × 512 (voxel size 0.39 × 0.39 × 0.5 mm). The source images were visualized with the aid of multiplanar reconstruction and maximal intensity projection using Osirix software (64-bit version 3.8; Pixmeo).

Diffusion-weighted imaging was obtained with 2 levels of diffusion sensitization (b values of 0 and 1000 seconds/mm^2), using a 4-mm thickness and a 1-mm gap. Two independent neuroradiologists, who were blinded to the type of stent used and the procedural details, analyzed the diffusion-weighted images for the number, size, and location of hyperintense signal changes (> 2 mm), including sidedness (ipsilateral/contralateral) relative to vascular territory subserved by the target stent. Any differences between the neuroradiologists in terms of lesion identification on diffusion-weighted images were identified, and disputed cases were adjudicated by consensus agreement reached by the 2 reviewers and the senior author after discussion of the case. Each lesion identified on diffusion-weighted imaging was then measured for diameter and location by using Osirix software, and its relative ipsilateral/contralateral relationship was identified with respect to the deployed stent.

Statistical Analysis

The differences in characteristics between subtypes were evaluated using 1-way ANOVA, the chi-square likelihood ratio test, and odds ratios for categorical values by using JMP version 8.02 (SAS Institute, Inc.). Statistical significance was assumed for $p < 0.05$. The means are expressed ± SD throughout.

Results

Fifty-eight patients underwent stent-mediated coil em-

Brought to you by Tufts University | Unauthenticated | Downloaded 11/15/26 12:59 PM UTC

bolization of intracranial aneurysms during the study period. All patients underwent 3-T MR angiography and diffusion-weighted imaging within 3 days of the procedure. Thirty-three patients (57%) underwent stent-mediated coil embolization performed using the Enterprise closed-cell design stent, and 25 (43%) underwent the same procedure performed using the Neuroform open-cell design stent for assistance in coil buttressing in wide-necked aneurysms. All treated aneurysms were unruptured, except for 1 case treated with a Neuroform stent.

Findings on MR Angiography and Identification of the Crescent Sign

We analyzed posttreatment 3-T MR angiographic imaging for evidence of incomplete stent apposition. Our review of posttreatment 3-T MR angiography of vessel segments containing closed-cell design Enterprise stents revealed an unusual flow signal outside of the susceptibility artifact of the stent struts (Fig. 2). This flow signal identified outside of the stent strut confines was noted in a large preponderance of cases treated with Enterprise stent–mediated coil embolization, and was dubbed the crescent sign based on its semilunar shape. Contemporaneous flat-panel CT imaging obtained at the time of the embolization procedure with and without contrast injection was carefully reviewed after overlay of corresponding cross-sections (Fig. 2B). Cross-sectional analysis confirmed that the crescent sign corresponds to an area where the Enterprise stent has failed to appose to the vessel wall following stent delivery and coil insertion, resulting in incomplete stent apposition (Fig. 2C). A crescent sign on 3-T MR angiography thus identifies the signal of blood flow crossing the outline of the stent struts (seen as a dark susceptibility line) into this crescentic, isolated region, and back across the stent struts into the distal vessel lumen (Fig. 2D).

Prevalence and Factors Related to the Crescent Sign

The crescent sign was observed on 3-T MR angiography in 18 (54.5%) of 33 patients whose aneurysms were treated with Enterprise closed-cell design stent-mediated coil insertion. In contrast, careful review using multiplanar maximum intensity projection of the 3-T MR angiography acquisitions failed to enable crescent sign detection in any of the 25 patients who underwent stent-mediated coil embolization with Neuroform open-cell design stents (Fig. 3A and B). Angiographic flat-panel CT imaging with and without contrast injection demonstrated uninterrupted flow through the lumen of the Neuroform stent without evidence of incomplete stent apposition, correlating with the 3-T MR angiographic imaging (Fig. 3C and D). Because there was no crescent sign present in the Neuroform subset, we focused on the Enterprise subset for evaluation of a possible association of crescent sign with demographic or technical characteristics (Table 1). The crescent sign was more likely to be found in Enterprise stents deposited in the ICA compared with other locations ($p = 0.034$); aneurysm size was not different among cases with and without the crescent sign (6.82 vs 7.4 mm, respectively). The use of the jailing technique was evaluated because of concerns that it could affect the Enterprise stent's ability to expand sufficiently to appose the wall after withdrawal of the coil delivery microcatheter; it was not found to be associated with postprocedural crescent sign ($p = 0.805$).

Correlation Between Crescent Sign and Procedural Diffusion-Weighted Imaging Change

Given the known link between thromboembolic events and incomplete stent apposition, we evaluated (Fig. 4) the presence of lesions ipsilateral (Fig. 4C) to the stent on diffusion-weighted imaging and the association of these lesions with the crescent sign. In the entire group (Enterprise and Neuroform cases), ipsilateral lesions on diffusion-weighted imaging were detected in 12 (21%) of 58 patients with the crescent sign (all Enterprise cases) and in 4 (6.9%) without it (3 Enterprise and 1 Neuroform) (OR 18, 95% CI 4.33–74.8; $p < 0.0001$). None of the patients suffered an irreversible clinical deficit attributed to the lesions noted on diffusion-weighted imaging by the time of discharge. Given the absence of the crescent sign in Neuroform cases and the low number of ipsilateral diffusion-weighted imaging findings in Neuroform cases (1 of 25), we limited subsequent analysis of the link between the crescent sign and lesions on diffusion-weighted imaging to the Enterprise subset to avoid bias, and to remove any undefined differences that may be attributable to the stent type (Table 2).

Within the Enterprise cohort, ipsilateral lesions were detected on diffusion-weighted imaging in 15 (45.5%) of 33 Enterprise-treated cases. The crescent sign was found to be strongly associated with lesions on ipsilateral diffusion-weighted imaging; the crescent sign was present in 12 (80%) and absent in 3 (20%) of 15 cases with lesions (OR 8, 95% CI 1.61–39.6; $p = 0.006$). In contrast, neither aneurysm location in the ICA ($p = 0.505$) nor aneurysm size ($p = 0.696$) was significantly correlated with lesions being found on diffusion-weighted imaging. Similarly, endovascular technique (jailing vs sequential), guide catheter type and number (single vs dual), intraprocedural anticoagulation, and pretreatment antiplatelet regimen were not statistically different.

Examination of the number and size distribution of ipsilateral lesions on diffusion-weighted imaging revealed a total of 60 lesions in the 12 patients with the crescent sign, compared with 3 lesions in the 3 patients without the crescent sign. The mean number of lesions per patient on diffusion-weighted imaging was 4.92 ± 7.5 in cases with the crescent sign (median 1.5), versus 1 ± 0 in cases without it (a single lesion in each patient) (Fig. 5 left); the mean lesion size was 4.13 ± 1.27 mm in cases with the crescent sign versus 3.78 ± 0.2 mm in cases without it ($p = 0.642$) (Fig. 5 right).

Discussion

Intracranial stents have advanced the treatment of wide-necked intracranial aneurysms,[7,9] and have enabled endovascular treatment of lesions previously relegated to the microsurgical technique.[13,15] Although recent studies have critically evaluated the rates of thromboembolic and ischemic events associated with stent-assisted coil embolization,[3,11] definite risk factors beyond inadequate antiplatelet regimen remain poorly defined.

Brought to you by Tufts University | Unauthenticated | Downloaded 11/15/26 12:59 PM UTC

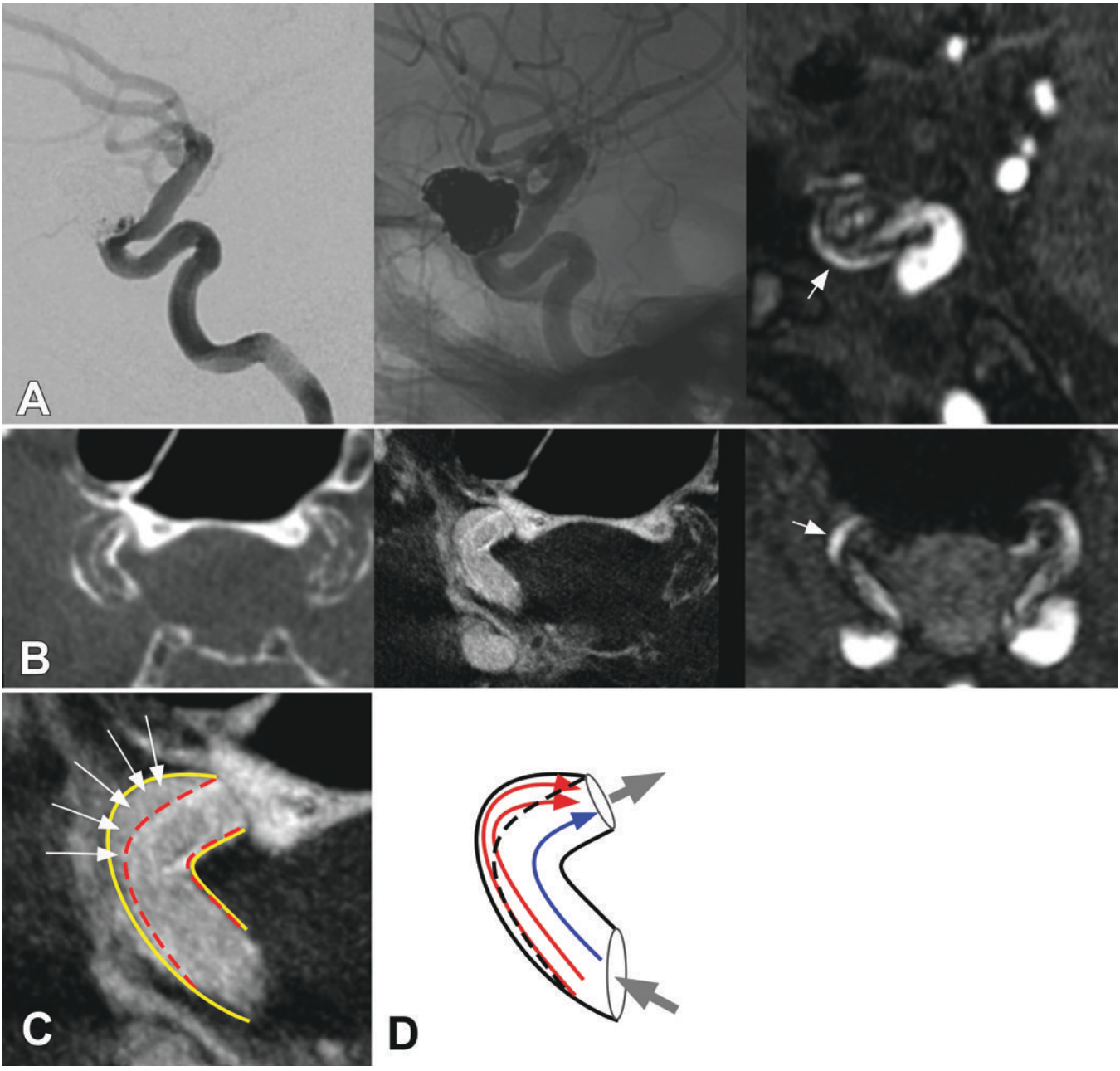


Fig. 2. **A:** Sagittal 3-T MR angiography study demonstrating the crescent sign (*arrow*, **right**) in a patient following Enterprise stent–assisted coil embolization of bilateral wide-necked carotid ophthalmic aneurysms. **B:** Axial high-resolution flat-panel CT scans obtained without **(left)** and with **(center)** contrast revealing Enterprise stents to be nonapposed to the vessel wall, with a corresponding crescent sign on axial 3-T MR angiography study (*arrow*, **right**). **C:** Magnified view of contrast-enhanced flat-panel CT scan outlines of right carotid vessel wall *(solid lines)*, stent struts *(dashed lines)*, and orphaned vessel lumen *(arrows)* resulting from the incomplete stent apposition. **D:** Schematic drawing of incomplete stent apposition showing arterial flow *(upper arrows)* through the stent struts *(dashed line)* into the crescent sign and back into vessel lumen.

We hypothesized that one of the causes of procedure-related thromboembolism during endovascular stent-mediated aneurysm embolization may be the result of incomplete stent apposition. Although incomplete stent apposition has been extensively studied in coronary and carotid artery intervention, its presence and implications remain undefined in intracranial stenting. Incomplete stent apposition in the coronary circulation appears to be more prevalent in drug-eluting stents,[1] a finding that was obtained using optical coherence tomography, and has been linked to late stent thrombosis and long-term occlusion,[4,17] adverse events that could have devastating sequelae in the cerebral circulation. These results suggest the need for continued long-term follow-up of patients after stent-mediated coil insertion for aneurysm treatment if they demonstrate incomplete stent apposition. The time course of incomplete stent apposition and any effect it may have on long-term thromboembolic events remain to be determined.

Brought to you by Tufts University | Unauthenticated | Downloaded 11/15/26 12:59 PM UTC

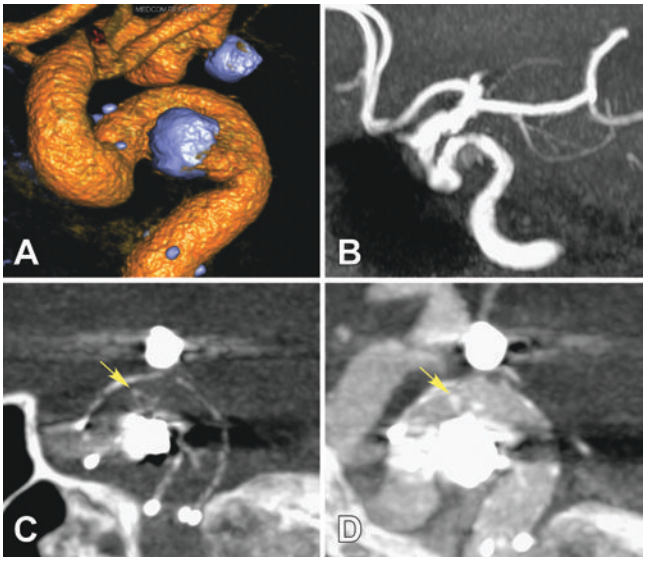


Fig. 3. Dual-volume 3D angiographic reconstruction of a wide-necked cavernous carotid aneurysm on a tight-radius 180° cavernous carotid bend **(A)**; the lesion was treated with Neuroform stent–assisted coil embolization. A 3-T MR angiography study **(B)** in corresponding projection failing to demonstrate the crescent sign. Flat-panel CT scans without **(C)** and with **(D)** addition of contrast agent showing the Neuroform stent struts to be apposed to the vessel wall, with no evidence of incomplete stent apposition, and identifying a focal instance of inner-curve fish-scaling *(arrow)*.

TABLE 1: Comparison of factors in patients with the crescent sign on 3-T MR angiography*

Factor	Crescent Sign Present	Crescent Sign Absent	p Value
stent type			
Neuroform open-cell design	0 (0%)	25 (100%)	
Enterprise closed-cell design	18 (54.5%)	15 (45.5%)	
Enterprise cohort			
no. of patients	18	15	
patient demographic data			
mean age (yrs)	59.6 ± 9.7	54.5 ± 10.2	0.150
M/F	4:14	2:13	0.505
mean BMI (kg/m^2)	28.1 ± 4.5	26.7 ± 6.2	0.467
aneurysm location in ICA	17	10	0.034
mean aneurysm size (mm)	6.82 ± 5.3	7.40 ± 3.2	0.707
procedural technique			
5 Fr catheter/6 Fr catheter	3:15	4:11	0.485
jailing/sequential technique	15:3	12:3	0.805

* The mean values are expressed ± SD.

The central finding of the current study is that the presence of incomplete stent apposition, as evidenced by the 3-T MR angiographic crescent sign within the intracranial circulation, is highly associated with an increased procedure-related risk of thromboembolic complications as demonstrated on diffusion-weighted imaging. In the current study we detected the crescent sign by using 3-T MR angiography, and we did not evaluate whether results could be obtained with similar sensitivity in lower-field-strength MR units (that is, 0.5–1.5 T) in clinical use. The concomitant use of intraprocedural high-resolution flat-panel CT scans with and without angiographic contrast enabled the identification and confirmation of the crescent sign as an indicator of incomplete stent apposition. Nonetheless, it is likely that the crescent sign on 3-T MR angiography is not sufficiently sensitive to detect all cases of incomplete stent apposition. Future work using flat-panel CT scanning may yield more information regarding the link between milder forms of incomplete stent apposition and lesions seen on diffusion-weighted imaging.

Although the 0% rate of crescent sign detection in patients treated with Neuroform stents could be the result of a difference in the susceptibility artifact of its slightly thicker struts (75 vs 60 μm), the data from contemporaneous flat-panel CT scanning argues against this possibility. Flat-panel CT analysis in available Neuroform-treated cases showed good stent apposition on both the inner and outer walls, even in tight-radius tortuosity, and was even sufficiently sensitive to detect the inner curve fish-scaling characteristic of the Neuroform design[6] (*arrows* in Figs. 1C and 3C). The single case of an ipsilateral lesion on diffusion-weighted imaging after Neuroform stent delivery occurred in a patient whose stent-mediated coil placement procedure was preceded by a 30-minute ipsilateral carotid balloon test occlusion: the stent was confirmed to be free of incomplete apposition on flat-panel CT, and of the crescent sign on 3-T MR angiography.

Given that the link between incomplete stent apposition and lesions on diffusion-weighted imaging was confined to the Enterprise cohort (since the Neuroform cohort had no detected crescent sign and a single lesion on diffusion-weighted imaging in 25 patients), the link between crescent sign and lesions seen on diffusion-weighted imaging cannot be attributed to issues of variability in stent design and/or delivery methods between Enterprise and Neuroform stents. Furthermore, analysis of the groups with and without lesions on diffusion-weighted imaging within the Enterprise subset showed no statistically significant difference in aneurysm location or size, guide catheter size, endovascular technique, or mean procedural ACT, identifying the presence of the crescent sign as the only predictor. The equality between the subgroups with respect to these variables demonstrates that it is unlikely that the results obtained in this study are confounded by undetected differences in treatment protocol. Additionally, although the dataset presented in this study was collected prospectively, the crescent sign was not identified until a review of the 3-T MR angiographic images was completed and analyzed, thus precluding a significant possibility that periprocedural treatment of patients with incomplete stent apposition differed from that of patients with well-apposed stents.

It is noteworthy that 20% of patients treated with the Enterprise device who did not have incomplete stent apposition demonstrated an ischemic lesion on diffusion-weighted imaging, whereas only 4% of patients who received the Neuroform stent and who did not have incom-

Brought to you by Tufts University | Unauthenticated | Downloaded 11/15/26 12:59 PM UTC

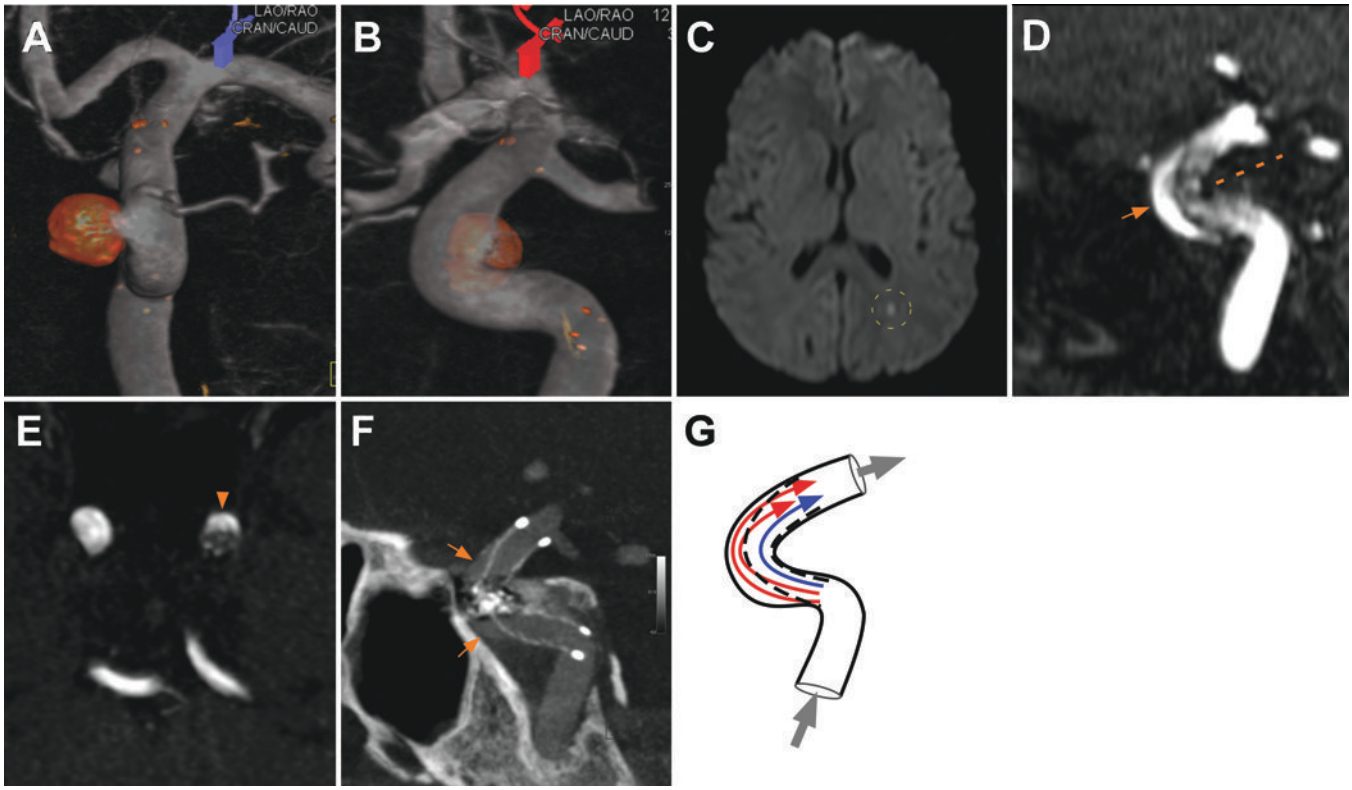


Fig. 4. Dual-volume 3D angiographic reconstruction, in anteroposterior **(A)** and lateral **(B)** projections, of a wide-necked left superior hypophyseal carotid aneurysm treated with Enterprise stent–assisted coil embolization. Postprocedural 3-T diffusion-weighted imaging study **(C)** revealing a high-intensity signal of restricted diffusion in the ipsilateral left corona radiata *(dashed circle)*. The crescent sign *(arrow and arrowhead)* is revealed on contemporaneous 3-T MR angiography studies obtained in the sagittal **(D)** and axial **(E)** projections, coincident with radiographic confirmation of incomplete stent apposition on contrast-enhanced flat-panel CT imaging **(F)** in the corresponding projection, highlighting orphaned vessel lumen *(arrows)*. Schematic drawing **(G)** of flow through the stent struts into the orphaned lumen corresponding to the crescent sign, and back into the distal vessel lumen.

plete stent apposition demonstrated such a lesion. This information probably indicates that there is an alternate etiology that predisposes patients receiving an Enterprise stent to periprocedural thromboembolism. One potential explanation is that milder forms of incomplete stent apposition may not be detectable by use of the crescent sign, because the orphaned lumen created by incomplete stent apposition is not sufficiently large to generate a signal on even the high field strength of 3-T MR angiography. Another possibility may be related to the high flow velocities a poorly apposed stent is subjected to in the middle of the vessel lumen, compared with the near-zero flow velocities of a well-apposed stent at the vessel wall. In contrast to the uncoated Neuroform stent, the Enterprise device is covered with a thin layer of Parylene coating material, which is a well-known biocompatible material used in certain stents and pacemakers (http://en.wikipedia.org/wiki/Parylene [accessed May 2, 2011]). One could hypothesize, although with no supporting evidence at this point, that the higher velocities to which a poorly apposed stent is exposed could interact with the Parylene coating and introduce the likelihood of fracture, shedding, and embolization of coating material. Clearly, further work remains to be done to elucidate the mechanism influencing the risk of thromboembolism associated with Enterprise stent delivery in aneurysm coil placement procedures.

The finding that 17 of 18 cases of crescent sign were detected in stents deposited in the relatively tortuous ICA suggests a possible link between target vessel anatomy and interaction with the architecture of the Enterprise closed-cell design stent. In fact, Tanigawa et al.[19] have demonstrated that stents with a closed-cell design used in coronary vessels are more susceptible to incomplete stent apposition than open-cell stents. Additional investigation into the interaction between the stent delivery mechanism and tortuous vessels needs to be undertaken to explain the high prevalence of incomplete stent apposition in cases treated with Enterprise devices.

Analysis of the size distribution and pattern of ipsilateral lesions on diffusion-weighted imaging (Fig. 5) appears to be consistent with an embologenic source association in the subset with the crescent sign, compared with a single lesion in each of the 3 patients without the crescent sign and associated incomplete stent apposition. Although the exact mechanism of the association between incomplete stent apposition and ipsilateral lesions on diffusion-weighted imaging cannot be ascertained from the current study, 1 of the following 2 mechanisms probably contributes: 1) high shear–induced platelet acti-

Brought to you by Tufts University | Unauthenticated | Downloaded 11/15/26 12:59 PM UTC

TABLE 2: Univariate analysis of factors and ipsilateral diffusion-weighted MR imaging changes in the Enterprise cohort*

Factor	Diffusion-Weighted Lesions		p Value
	Present	Absent	
total patient count	15	18	
presence of crescent sign	12	6	0.006
patient demographic data			
mean age (yrs)	59.2 ± 8.3	55.6 ± 11.3	0.306
M/F	2:13	4:14	0.505
mean BMI (kg/m^2)	27.6 ± 4.1	27.3 ± 6.2	0.864
aneurysms located in ICA	13	14	0.505
mean aneurysm size (mm)	7.42 ± 5.7	6.81 ± 3.1	0.696
procedural technique			
5 Fr catheter/6 Fr guide catheter	3:12	4:14	0.876
single/dual guide catheters	14:1	17:1	0.894
jailing/sequential technique	12:3	15:3	0.805
comorbidities			
hypertension	10	12	1.00
diabetes mellitus	0	0	NA
hyperlipidemia	6	7	0.948
history of tobacco use	11	16	0.247
current tobacco use	5	8	0.514
current alcohol use	4	5	0.943
coronary artery disease	0	1	0.266
peripheral vascular disease	2	2	0.846
medications at time of procedure			
proton pump inhibitor	2	5	0.304
aspirin pretreatment	15	18	NA
clopidogrel pretreatment	15	18	NA
heparin dose/BMI†	178 ± 69	190 ± 57	0.575
mean procedural ACT (seconds)	239 ± 17	233 ± 10	0.236

* NA = not applicable.
† Units are expressed as USP*m^2/kg.

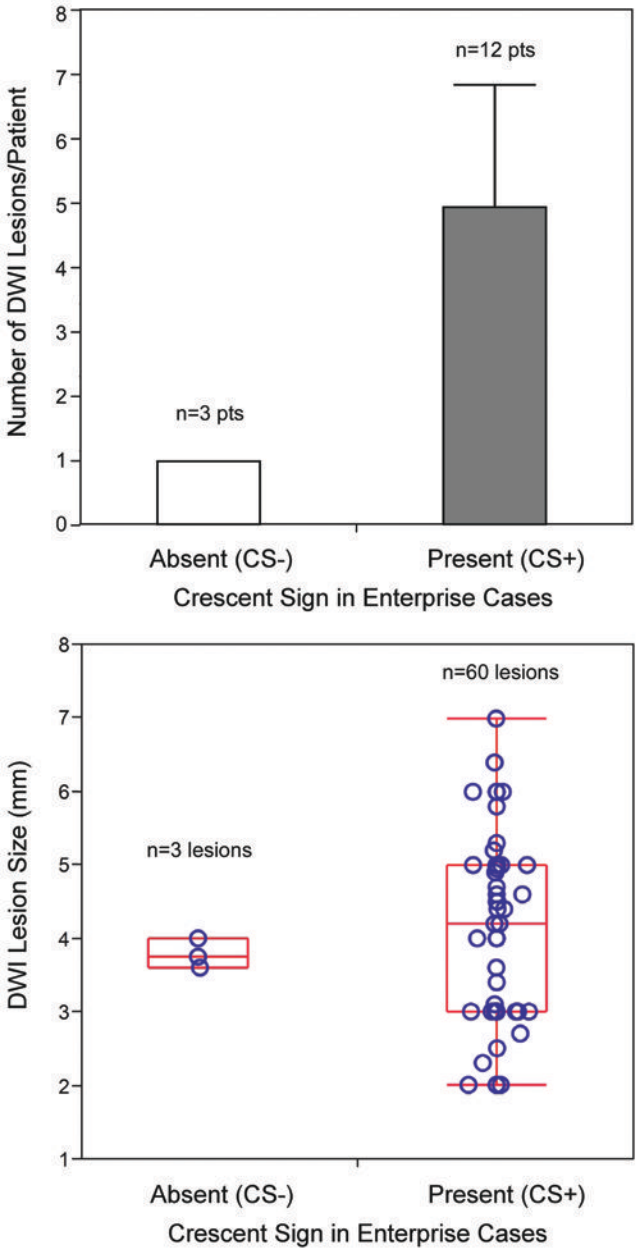


Fig. 5. Analysis of postprocedural lesions revealed on diffusion-weighted imaging (DWI) in patients (pts) undergoing coil embolization with the aid of an Enterprise stent. **Upper:** Number of lesions per patient based on the presence (CS+) or absence (CS–) of crescent sign on 3-T MR angiography. **Lower:** Size distribution of ipsilateral lesions on diffusion-weighted imaging based on crescent sign status.

vation and plug formation resulting from the high velocity of blood flow and its formed elements striking the stent struts during the blood's ingress and egress into the orphaned unapposed crescentic region of incomplete stent apposition; and 2) formation of thrombus in the low-flow recesses at the edges of the orphaned crescentic region of incomplete stent apposition, followed by distal migration and subsequent embolization downstream. Research is needed to elucidate stent and vessel characteristics that create a predisposition to incomplete stent apposition, and the fluid mechanics of malapposed stent struts within tortuous vessels. Future analysis, including computational fluid dynamic modeling, is needed to determine the local microhemodynamic conditions and their possible effect on thrombus formation and platelet activation. Such understanding may help in identifying the mechanism of the association between incomplete stent apposition and periprocedural thromboembolism, to avoid its occurrence and help mitigate its short- and long-term sequelae.

Conclusions

The central finding of this study is that incomplete apposition of the Enterprise closed-cell design stent to the vessel wall is associated with an increased risk of thromboembolic events following stent-mediated coil embolization of intracranial aneurysms. Incomplete stent apposition was only found with the Enterprise device, and is

Brought to you by Tufts University | Unauthenticated | Downloaded 11/15/26 12:59 PM UTC

detectable by use of the crescent sign on 3-T MR angiography. Further work is needed to elucidate the mechanism that predisposes Enterprise stents to malapposition to the vessel wall, and the potential long-term sequelae of this phenomenon.

Disclosure

Dr. Malek has received unrestricted research support from Codman Neurovascular, Inc., and Boston Scientific Corp. unrelated to the current study. The authors report no conflict of interest concerning the materials or methods used in this study or the findings specified in this paper.

Author contributions to the study and manuscript preparation include the following. Conception and design: Malek. Acquisition of data: all authors. Analysis and interpretation of data: Malek, Heller. Drafting the article: Malek, Heller. Critically revising the article: Malek, Heller. Statistical analysis: Malek, Heller. Administrative/technical/material support: Malek. Study supervision: Malek.

Acknowledgment

The authors thank Courtney Petersen, P.A., for her assistance.

References

1. Barlis P, Regar E, Serruys PW, Dimopoulos K, van der Giessen WJ, van Geuns RJ, et al: An optical coherence tomography study of a biodegradable vs. durable polymer-coated limus-eluting stent: a LEADERS trial sub-study. **Eur Heart J 31:**165–176, 2010
2. Benndorf G, Claus B, Strother CM, Chang L, Klucznik RP: Increased cell opening and prolapse of struts of a neuroform stent in curved vasculature: value of angiographic computed tomography: technical case report. **Neurosurgery 58 (4 Suppl 2):**ONS-E380, 2006
3. Brooks NP, Turk AS, Niemann DB, Aagaard-Kienitz B, Pulfer K, Cook T: Frequency of thromboembolic events associated with endovascular aneurysm treatment: retrospective case series. **J Neurosurg 108:**1095–1100, 2008
4. Cook S, Wenaweser P, Togni M, Billinger M, Morger C, Seiler C, et al: Incomplete stent apposition and very late stent thrombosis after drug-eluting stent implantation. **Circulation 115:**2426–2434, 2007
5. Cronqvist M, Wirestam R, Ramgren B, Brandt L, Nilsson O, Säveland H, et al: Diffusion and perfusion MRI in patients with ruptured and unruptured intracranial aneurysms treated by endovascular coiling: complications, procedural results, MR findings and clinical outcome. **Neuroradiology 47:**855–873, 2005
6. Ebrahimi N, Claus B, Lee CY, Biondi A, Benndorf G: Stent conformity in curved vascular models with simulated aneurysm necks using flat-panel CT: an in vitro study. **AJNR Am J Neuroradiol 28:**823–829, 2007
7. Gounis MJ, DeLeo MJ III, Wakhloo AK: Advances in interventional neuroradiology. **Stroke 41:**e81–e87, 2010
8. Grunwald IQ, Papanagiotou P, Politi M, Struffert T, Roth C, Reith W: Endovascular treatment of unruptured intracranial aneurysms: occurrence of thromboembolic events. **Neurosurgery 58:**612–618, 2006
9. Henkes H, Bose A, Felber S, Miloslavski E, Berg-Dammer E, Kühne D: Endovascular coil occlusion of intracranial aneurysms assisted by a novel self-expandable nitinol microstent (neuroform). **Interv Neuroradiol 8:**107–119, 2002
10. Irie K, Negoro M, Hayakawa M, Eayashi J, Kanno T: Stent assisted coil embolization: the treatment of wide-necked, dissecting, and fusiform aneurysms. **Interv Neuroradiol 9:**255–261, 2003
11. Ishibashi T, Murayama Y, Saguchi T, Ebara M, Irie K, Takao H, et al: Thromboembolic events during endovascular coil embolization of cerebral aneurysms. **Interv Neuroradiol 12 (Suppl 1):**112–116, 2006
12. Lee YJ, Kim DJ, Suh SH, Lee SK, Kim J, Kim DI: Stent-assisted coil embolization of intracranial wide-necked aneurysms. **Neuroradiology 47:**680–689, 2005
13. Mocco J, Hanel RA, Sharma J, Hauck EF, Snyder KV, Natarajan SK, et al: Use of a vascular reconstruction device to salvage acute ischemic occlusions refractory to traditional endovascular recanalization methods. Clinical article. **J Neurosurg 112:**557–562, 2010
14. Mocco J, Snyder KV, Albuquerque FC, Bendok BR, Boulos AS, Carpenter JS, et al: Treatment of intracranial aneurysms with the Enterprise stent: a multicenter registry. Clinical article. **J Neurosurg 110:**35–39, 2009
15. Piotin M, Blanc R, Spelle L, Mounayer C, Piantino R, Schmidt PJ, et al: Stent-assisted coiling of intracranial aneurysms: clinical and angiographic results in 216 consecutive aneurysms. **Stroke 41:**110–115, 2010
16. Richter G, Engelhorn T, Struffert T, Doelken M, Ganslandt O, Hornegger J, et al: Flat panel detector angiographic CT for stent-assisted coil embolization of broad-based cerebral aneurysms. **AJNR Am J Neuroradiol 28:**1902–1908, 2007
17. Siqueira DA, Abizaid AA, Costa Jde R, Feres F, Mattos LA, Staico R, et al: Late incomplete apposition after drug-eluting stent implantation: incidence and potential for adverse clinical outcomes. **Eur Heart J 28:**1304–1309, 2007
18. Soeda A, Sakai N, Murao K, Sakai H, Ihara K, Yamada N, et al: Thromboembolic events associated with Guglielmi detachable coil embolization with use of diffusion-weighted MR imaging. Part II. Detection of the microemboli proximal to cerebral aneurysm. **AJNR Am J Neuroradiol 24:**2035–2038, 2003
19. Tanigawa J, Barlis P, Dimopoulos K, Dalby M, Moore P, Di Mario C: The influence of strut thickness and cell design on immediate apposition of drug-eluting stents assessed by optical coherence tomography. **Int J Cardiol 134:**180–188, 2009
20. Wakhloo AK, Mandell J, Gounis MJ, Brooks C, Linfante I, Winer J, et al: Stent-assisted reconstructive endovascular repair of cranial fusiform atherosclerotic and dissecting aneurysms: long-term clinical and angiographic follow-up. **Stroke 39:**3288–3296, 2008
21. Wells-Roth D, Biondi A, Janardhan V, Chapple K, Gobin YP, Riina HA: Endovascular procedures for treating wide-necked aneurysms. **Neurosurg Focus 18(2):**E7, 2005

Manuscript submitted December 6, 2010.
Accepted April 19, 2011.
Please include this information when citing this paper: published online May 27, 2011; DOI: 10.3171/2011.4.JNS102050.

Address correspondence to: Adel M. Malek, M.D., Ph.D., Department of Neurosurgery, Tufts Medical Center, 800 Washington Street, Proger 7, Box 178, Boston, Massachusetts 02111. email: amalek@tuftsmedicalcenter.org.

Brought to you by Tufts University | Unauthenticated | Downloaded 11/15/26 12:59 PM UTC